Journal of the Korean Physical Society, Vol. 66, No. 1, January 2015, pp. 92∼95

Enhanced Bandwidth of a Microstrip Antenna Using a Parasitic Mushroom-like Metamaterial Structure for Multi-robot Cooperative Navigation

Cherl-Hee Lee
College of IT Engineering, Kyungpook National University, Daegu 702-701, Korea

Jonghun Lee,* Yoon-Gu Kim and Jinung An
Robotics Research Division, Daegu Gyeongbuk Institute of Science & Technology, Daegu 711-813, Korea

(Received 8 December 2013, in final form 1 July 2014)

The broadband design of a microstrip patch antenna is presented and experimentally studied for multi-robot cooperation. A parasitic mushroom-like metamaterial (MTM) patch close to a microstrip top patch is excited through gap-coupling, thereby producing a resonance frequency. Because of the design, the resonance frequency of the parasitic MTM patch is adjacent to that of the main patch, and the presented antenna can achieve an enhanced bandwidth of 450 MHz, which is about two times the bandwidth of a conventional patch antenna without the MTM parasitic patch. The error rate of packet transmissions for measuring the distance between a leader robot and a follower robot was also improved by almost two-fold.

PACS numbers: 41.20.Jb, 84.40.Ba, 81.40.Rs, 84.40.-x
Keywords: Metamaterials, Mushroom, Parasitic, Multi-robot
DOI: 10.3938/jkps.66.92

I. INTRODUCTION

Intelligent remote-controlled multi-robots have received considerable attention over the past decade in the scientific and engineering communities [1, 2]. The most important technical challenge of remote control is to secure reliable and robust wireless communication in both indoor and unstructured environments where communication infrastructures are poor. Remote-controlled multi-robots navigate cooperatively and visit adverse environments such as disaster sites with the task of rescuing survivors. A wireless communication system for multi-robot cooperative navigation consists of a leader robot, follower robots, and interfaces for remote control. Each follower robot has a wireless router using the standard Transmission Control Protocol/Internet Protocol (TCP/IP), and communicates with the leader robot or other following robots while keeping a valid distance by the received signal strength indication (RSSI). However, in both indoor and unstructured environments where communication is hindered, robots may have to tolerate low signal-to-noise ratios and temporary losses of communication connectivity along with constraints on power and bandwidth. Highly-efficient, wideband antennae have, thus, been developed to provide robust and reliable distance-keeping cooperative navigation.

Microstrip patch antennae have been widely used in military (aircraft, spacecraft, satellites, radars, and missiles) and commercial (mobile radios and wireless communication systems) applications [3,4]. Printed antennae have many attractive features, such as light weight, small size, low cost, mechanical robustness, and ease of fabrication. In addition, they can be easily integrated with planar surfaces and have many degrees of freedom in their design. However, classical microstrip patch antennae inherently have narrow frequency bandwidths, typically 1 $\sim$ 5%, which is a major factor limiting widespread applications. Several methods, such as stacked patches and coplanar parasitic patches, have been developed in order to increase the bandwidth of microstrip antennae, in addition to common techniques of increasing patch height and decreasing substrate permittivity [5,6]. The stacked patches and the conventional techniques have solved the bandwidth problem for a relatively-large antenna thickness, because the bandwidth is generally proportional to the antenna's thickness measured in wavelengths. However, a practical limit exists on increasing the antenna's thickness; if it is increased beyond 0.1λ, surface-wave propagation takes place, resulting in degraded antenna performance. Another popular bandwidth extension technique is the use of parasitic patches

*E-mail: jhlee@dgist.ac.kr

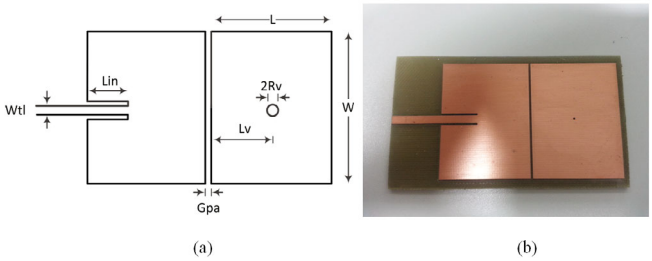

Fig. 1. (Color online) ZOR mushroom antennae with a mushroom-like MTM parasitic patch: (a) structure and (b) photo.

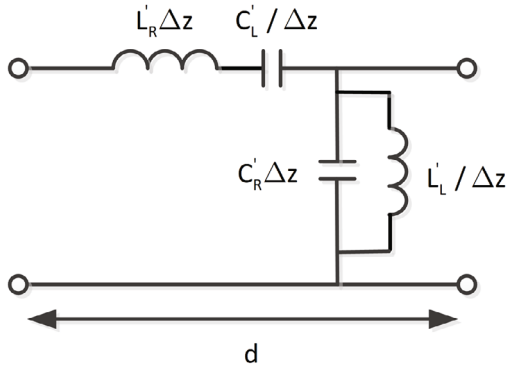

Fig. 2. Circuit model of the presented antenna.

without increasing the volume or degrading the performance of low-profile antennas [7, 8]. A parasitic patch placed close to the fed main patch is excited through coupling with fringing fields along the width between the two patches. If the resonance frequencies of these two patches are close to each other, then the neighboring resonance frequencies will provide a broader bandwidth than that of a single patch.

Recently, metamaterials (MTMs) having simultaneously negative permittivity (ε) and permeability (μ), commonly referred to as left-handed materials (LHMs), have received considerable attention in the antenna communities because they reduce antenna size and enhance narrow bandwidths [9–12]. In particular, mushroom-like MTM structures fabricated on microstrip patch substrates possess exciting properties, including suppression of surface-wave propagation, high surface impedance for both TE and TM polarizations, and compactness. These features help to improve the antenna's performance by increasing the antenna's gain and reducing back radiation [13–15]. Upon this background, this paper presents a new parasitic mushroom-like MTM structure to improve the bandwidth and the radiation efficiency. The parasitic patch using the mushroom-like MTM can produce a resonance frequency adjacent that of the main patch to enhance the bandwidth. It can also suppress surface waves on the gap-coupled parasitic patch for improved radiation efficiency in a specific frequency band. In this study, the parasitic patch provides a resonance frequency adjacent to that of the main patch, and the bandwidth was thereby enhanced up to 2 times that of a microstrip antenna without a parasitic patch. Furthermore, the gain was also increased by up to two-fold by using a parasitic patch having the same size as the main patch.

II. ANTENNA DESIGN

MTMs are effective homogeneous structures that can be modeled with one-dimensional transmission lines (TLs) as composite right/left-hand (CRLH) structures under the condition that the average cell size is smaller than the guided wavelength. A general CRLH TL unit-cell consists of a series capacitance and a shunt inductance, as well as a series inductance and a shunt capacitance [9].

Figure 1 shows the presented microstrip antenna with a mushroom-like MTM parasitic patch. The mushroom structure is built with a rectangular top patch and a metal via connecting the top patch to the ground. The gap between neighboring patches represents the left-handed series capacitance, and the vertical via of the top plate acts as the left-handed shunt inductance in the equivalent circuit model, while the shunt capacitance and series inductance, representing the right-handed TL, are due to parasitic effects caused by the microstrip geometry. For impedance matching with a 50-Ω microstrip transmission line, we used an inset microstrip feed line with a width (W_{tl}) and a length (L_{in}) of 3 mm and 13 mm, respectively. The widths (W) and the lengths (L) of both the main patch and the parasitic patch of the presented antenna were 42 mm and 32 mm, respectively; the via's diameter ($2R_v$) was 0.6 mm, and the height and the relative permittivity of the substrate (FR4) were 1.6 mm and 4.4, respectively.

The CRLH TL model can be represented as a combination of a per-unit-length series inductance (L'_R), a per-unit-length shunt capacitance (C'_R), a times-unit-length shunt inductance (L'_L), and a times-unit-length series capacitance (C'_L), as shown in Fig. 2. According to lossless transmission line theory, the propagation constant of a CRLH TL is given by $\gamma = j\beta = \sqrt{Z'Y'}$, where Z′ and Y′ are the per-unit-length impedance and the per-unit-length admittance, respectively. Z′ and Y′ are obtained as [9]

$$\begin{aligned} Z'(\omega) &= \frac{Z(\omega)}{\Delta z} = j\left(\omega L'_R - \frac{1}{\omega C'_L}\right), \\ Y'(\omega) &= \frac{Y(\omega)}{\Delta z} = j\left(\omega C'_R - \frac{1}{\omega L'_L}\right). \end{aligned} \tag{1}$$

The series resonance frequency and the shunt resonance frequency are given as $\omega_{se} = 1/\sqrt{L'_R C'_L}$ and $\omega_{sh} = 1/\sqrt{L'_L C'_R}$, respectively. According to the equivalent one-dimensional open-ended CRLH TL unit-cell, the dispersion relation related to Bloch-Floquet theory [9] is

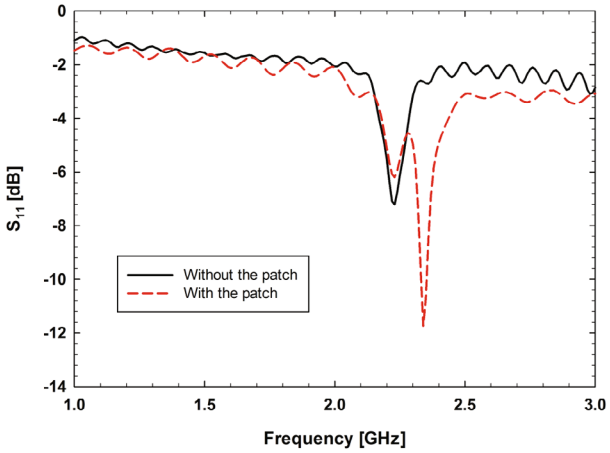

Fig. 3. (Color online) S_{11} parameter as a function of the frequency.

obtained as follows:

$$\cos\beta d = 1 - \frac{1}{2}\left\{\frac{\omega^2}{\omega_{RH}^2} + \frac{\omega_{LH}^2}{\omega^2} - \left(\frac{1}{\omega_{sh}^2} + \frac{1}{\omega_{se}^2}\right)\omega_{LH}^2\right\}, \quad (2)$$

where $\omega_{RH} = 1/\sqrt{L'_R C'_R}$ and $\omega_{LH} = 1/\sqrt{L'_L C'_L}$ With the resonant condition $\beta_m L = \mathrm{m}\pi$, β can be obtained for each resonance mode of $m = 0, \pm1, \pm2, \pm3, \ldots, \pm(N-1)$ of a N-cell CRLH TL with a total length L = N × d, where d is the length of the unit cell.

Figure 3 shows the S_{11} parameters of the presented antennae with and without the parasitic patch. A network analyzer (Agilent, PNA-X N5247A) was used to measure the return losses, the S_{11} parameters, which can show the frequency bandwidth. The resonance mode of the main patch was scaled to operate at 2.22 GHz, and the resonance frequency of the parasitic patch corresponded to 2.34 GHz. The 3-dB bandwidth of the presented antenna is 450 MHz, which is between 2.05 GHz and 2.5 GHz. The 3-dB bandwidth was enhanced by approximately two times relative to that of a conventional rectangular mushroom antenna without the parasitic patch.

The simulated radiation patterns of the presented antennae with and without the MTM parasitic patch are plotted in Fig. 4 on the E plane at 2.1 GHz. When the parasitic MTM patch is used, the main lobe's magnitude is 7 dBi, and the 3-dB angular width is 73.3 degrees, while for the conventional antenna without the patch, the main lobe magnitude is 6.1 dBi, and the 3-dB angular width is 79.9 degrees. The simulated radiation pattern was obtained by using a full-wave electromagnetic simulation with a high-frequency structure simulator (CST).

Figure 5 shows the tracking experimental setup for multi-robot cooperative navigation with a leader and a follower robot. The leader and the single follower robot are two-wheeled mobile robots and are equipped with a digital image sensor, a position-sensitive device sensor, a wireless router using the standard TCP/IP protocol, and

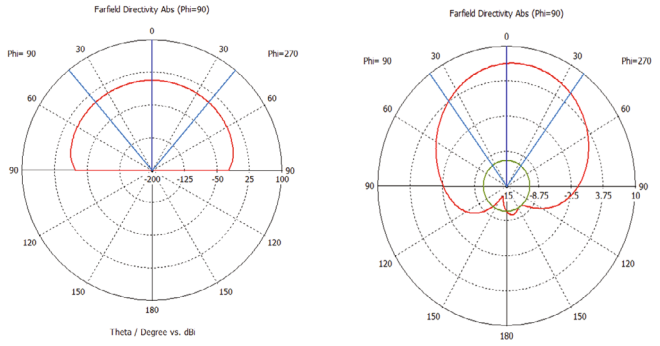

(a) (b)

Fig. 4. (Color online) Simulated radiation pattern (a) with and (b) without the MTM parasitic patch.

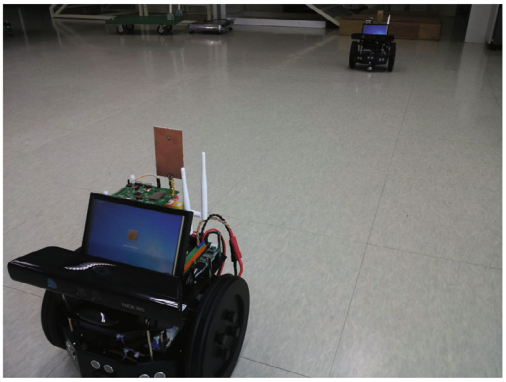

Fig. 5. (Color online) Two-wheeled mobile follower robot tracking a leader robot.

the presented antenna. While the leader robot is operated by a remote controller, the follower robot calculates the distance from the leader robot by using SDS-TWR (symmetrical double-sided two way ranging), and determines the bearing and following speed by estimating and tracking the moving leader robot with an image processing procedure based on the color and pattern information on the moving leader robot. The distance of SDS-TWR can be estimated by calculating the time difference between sending and receiving of an RF signal. Figure 5 shows an experimental environment in which the range between the leader robot and the follower robot is measured. Both robots navigate with a navigation speed of 10 cm/s and the interval between the two robots is measured and acquired for up to 500 times.

As shown in the graphs of Fig. 6, the initial intervals of 1, 2, 3, 4, and 5 m between the two robots are calculated, including an offset distance of about 2 m. The offset can be regarded as a stationary delay for calculating the ToF (time of flight). The ToFs over a specific threshold are considered as transmission errors, and they are displayed according to each maximum distance value in the graph. The experimental results for each interval measurement show a transmission error rate of less than 3.6%, which is

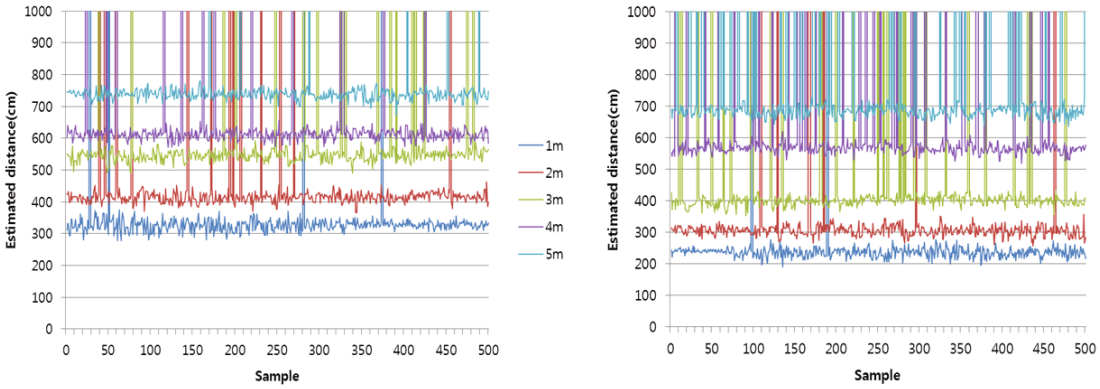

Fig. 6. (Color online) TDOA distance measurement from a leader robot to a follower robot (a) with and (b) without the MTM parasitic patch.

improved by almost two times relative to the 7.8% error rate for a conventional microstrip antenna without the MTM parasitic patch.

III. CONCLUSION

In this paper, for multi-robot cooperation, we present a bandwidth-enhanced microstrip patch antenna based on a parasitic MTM structure implemented by using a mushroom-shaped surface. The size and the height of the parasitic mushroom-like surface were designed to place the resonance frequency (2.34 GHz) near the resonant frequency (2.22 GHz) of the main patch in order to widen the small bandwidth. The presented antenna with the MTM parasitic patch achieved a 450 MHz 3-dB bandwidth, representing a roughly two-fold enhancement relative to the bandwidth of a conventional rectangular patch antenna without the MTM parasitic patch. The error rate of packet transmissions for measuring the distance between a leader robot and a follower robot was also improved by almost two-fold.

ACKNOWLEDGMENTS

This work was supported by the DGIST R&D Program of the Ministry of Science, ICT and Technology of Korea(14-RS-01). This work was also supported by the DGIST R&D Program of the Ministry of Science, ICT and Technology of Korea(14-BD-01).

REFERENCES

[1] Y.-G. Kim, J. An, K.-D. Kim, Z.-G. Xu and S.-G. Lee, *Advances in swarm intelligence Lecture notes in Computer Science*, Volume 6729, Xth ed (Springer, Berlin, 99, 2011).
[2] A. K. Sadek, Z. Han and K. J. R. Liu, IEEE Trans. Mobile Computing **9**, 505 (2010).
[3] S. K. Sharma, N. Jacob and L. Shafai, *Proc. IEEE AP-S Int Symp.*, 390 (2002).
[4] H. G. Akhavan and D. M. Syahkal, Electron. Lett. **30**, 1902 (1994).
[5] T. Huynh and K. F. Lee, Electron. Lett. **31**, 1310 (1995).
[6] R. Q. Lee, K. F. Lee and J. Bobinchak, Electron. Lett. **23**, 1070 (1987).
[7] A. Yu and X. Zhang, AP-Society Int. Symposium IEEE, 228 (2002).
[8] P. B. Parmar, B. J. Makwana and M. A. Jajal, Int. Conf. Comm. Syst. Network Technol., 53 (2012).
[9] C. Caloz and T. Itoh, IEEE Microwave Wireless Comp. Lett. **14**, 274 (2004).
[10] F. P. Casares-Miranda, C. Camacho-penalosa and C. Caloz, IEEE Trans. Antennas Propagat. **54**, 2292 (2006).
[11] C.-H. Lee, J. Lee, D.-S. Woo and K.-W. Kim, J. Korean Physical Soc. **61**, 1633 (2012).
[12] S. Kahng and G. Jang, Journal of Electromagnetic Engineering and Science **13**, 263 (2013).
[13] L. Liang, C. H. Liang and X. Chen, Microw. Opt. Technol. Lett. **50**, 2167 (2008).
[14] D. F. Sievenpiper, Ph.D. dissertation, UCLA, 1999.
[15] F. Yang and Y. R. Samii, IEEE Trans. Antennas Propagat. **51**, 2936 (2003).